Regenerative Therapy 28 (2025) 301–313

Contents lists available at ScienceDirect

Regenerative Therapy

journal homepage: http://www.elsevier.com/locate/reth

Original Article

Canine adipose-derived mesenchymal stromal cells inhibit the growth of canine hematologic malignancy cell lines

Yuyo Yasumura [a], Takahiro Teshima [a, b, *], Tomokazu Nagashima [c], Masaki Michishita [c], Hiroki Shigechika [a], Yoshiaki Taira [a], Ryohei Suzuki [a], Hirotaka Matsumoto [a]

[a] Laboratory of Veterinary Internal Medicine, School of Veterinary Medicine, Nippon Veterinary and Life Science University, Musashino, Tokyo 180-8602, Japan
[b] Research Center for Animal Life Science, Nippon Veterinary and Life Science University, Musashino, Tokyo 180-8602, Japan
[c] Laboratory of Veterinary Pathology, School of Veterinary Medicine, Nippon Veterinary and Life Science University, Musashino, Tokyo 180-8602, Japan

ARTICLE INFO

Article history:
Received 15 October 2024
Received in revised form
11 December 2024
Accepted 26 December 2024

Keywords:
Canine
Mesenchymal stromal cells
Lymphoma
Leukemia
Chronic inflammatory enteropathy
Safety

ABSTRACT

Introduction: Intestinal lymphoma may be latent in some dogs with chronic inflammatory enteropathy. Mesenchymal stromal cells (MSCs) have potential therapeutic applications for refractory chronic inflammatory enteropathy, but their impact on the development of potential intestinal lymphomas has not yet been evaluated. Therefore, this study was performed to investigate the effect of canine adipose-derived MSCs (cADSCs) on the growth of canine lymphoma cell lines to assess the safety of MSC-based therapy in terms of pro- and anti-tumorigenic effects.
Methods: CADSCs were co-cultured with canine lymphoma/leukemia cell lines of various lineages, with or without cell-to-cell contact, to evaluate their effects on proliferation, apoptosis, and cell cycle progression in vitro. Additionally, a bioluminescent canine lymphoma cell line, established through firefly luciferase transduction, was co-injected with varying doses of cADSCs into immunocompromised mice. The growth of canine lymphoma cells was monitored over time in vivo using bioluminescence imaging.
Results: CADSCs inhibited the proliferation of all canine lymphoma/leukemia cell lines in a dose-dependent manner in vitro, under conditions allowing cell-to-cell contact. This inhibition occurred via the induction of apoptosis, G0/G1 phase cell cycle arrest, or both mechanisms. However, these effects were lost when the cells were physically separated using Transwell inserts. In xenotransplantation mouse models, cADSCs dose-dependently inhibited canine lymphoma cell growth and lung metastasis, as indicated by reduced bioluminescence signals.
Conclusions: This study has demonstrated for the first time that cADSCs inhibit the growth of different lineages of canine lymphoma/leukemia cells both in vitro and in vivo. These findings suggest that MSC-based cell therapy could potentially be applied to canine chronic inflammatory enteropathy without increasing the risk of promoting the growth of latent intestinal lymphomas.

1. Introduction

Mesenchymal stromal cells (MSCs) have been extensively studied in both human and veterinary medicine as a promising cell source for treating various diseases, including chronic inflammatory conditions. MSCs exert anti-inflammatory, immunomodulatory, and angiogenic effects mediated by membrane molecules and soluble factors such as cytokines and growth factors. Diseases that naturally occur in companion animals, such as dogs, may better reflect the complex genetic, environmental, and physiological variations seen in humans, making them clinically relevant models for human disease and an important bridge between basic and preclinical research and human clinical trials [1]. To date, clinical trials in veterinary medicine have shown that MSCs have therapeutic effects in dogs with joint, spinal, neuromuscular, skin, gastrointestinal, and ocular diseases [2]. However, many safety concerns must be addressed before MSC-based therapies can be integrated into veterinary clinical practice. One of the major

* Corresponding author. Laboratory of Veterinary Internal Medicine, School of Veterinary Medicine, Nippon Veterinary and Life Science University, Musashino, Tokyo 180-8602, Japan.
E-mail addresses: d2203@nvlu.ac.jp (Y. Yasumura), teshima63@nvlu.ac.jp (T. Teshima), d2202@nvlu.ac.jp (T. Nagashima), michishita@nvlu.ac.jp (M. Michishita), v20037@nvlu.ac.jp (H. Shigechika), v18039@nvlu.ac.jp (Y. Taira), ryoheisuzuki@nvlu.ac.jp (R. Suzuki), matsumoto@nvlu.ac.jp (H. Matsumoto).
Peer review under responsibility of the Japanese Society for Regenerative Medicine.

https://doi.org/10.1016/j.reth.2024.12.019

Abbreviations

ALL	acute lymphoblastic leukemia
BCL	B-cell lymphoma
BMSCs	bone marrow-derived mesenchymal stromal cells
cADSCs	canine adipose-derived mesenchymal stromal cells
CCR	chemokine receptor
CDK	cyclin-dependent kinase
CIE	chronic inflammatory enteropathy
DMEM	Dulbecco's Modified Eagle's Medium
fLuc	firefly luciferase
HIF	hypoxia-inducible factor
LL	lymphoma/leukemia
MSCs	mesenchymal stromal cells
OD	optical density
PBS	phosphate-buffered saline
PI	propidium iodide
pRb	retinoblastoma protein
TCL	T-cell lymphoma
TGF-β	transforming growth factor-β
TIMP	tissue inhibitors of metalloproteinase
UCMSCs	umbilical cord-derived mesenchymal stromal cells

concerns is that MSCs may affect, or even promote, the development of malignancies in patients.

Accumulating evidence suggests that human MSCs may promote the development of various solid malignancies, including breast cancer, through mechanisms such as differentiation into tumor-associated fibroblasts, suppression of immune responses, promotion of tumor angiogenesis, stimulation of epithelial–mesenchymal transition, formation of a tumor-supportive microenvironment, and inhibition of tumor cell apoptosis [3–5]. Although few studies in veterinary medicine have explored the effects of MSCs on malignant tumor cells, our group previously demonstrated that canine adipose-derived MSCs (cADSCs) promoted the proliferation and invasion of a canine hepatocellular carcinoma cell line in vitro [6]. Conversely, many studies have shown that human MSCs inhibit the development of malignancies such as Kaposi's sarcoma by increasing inflammatory infiltration, inhibiting tumor angiogenesis, suppressing Wnt and Akt signaling, modulating the cell cycle, and inducing apoptosis of tumor cells [3,7]. Thus, MSCs appear to play a dual role in tumor development, exerting either pro- or anti-tumorigenic effects depending on various factors, including the source of the MSCs and the type of tumor. To ensure the success of MSC-based therapies without promoting potential malignancies, it is crucial to study the interactions between MSCs and different tumor cell types in detail.

Chronic inflammatory enteropathy (CIE) is a spontaneous gastrointestinal disorder in dogs that resembles inflammatory bowel disease in humans. It is characterized by chronic gastrointestinal symptoms lasting more than 3 weeks and inflammatory cell infiltration of the intestinal mucosa. The condition has multiple etiologies, including genetic and environmental factors, disturbances in the gut microbiota, and immune dysregulation [8]. Standard treatments for dogs with CIE include dietary therapy, antibiotics, and corticosteroids, but approximately 5 %–27 % of dogs do not respond to these treatments and have a poor prognosis [9]. MSC-based therapy is being considered for refractory CIE in dogs, with promising therapeutic effects of cADSCs reported in both preclinical and clinical studies [10,11]. Notably, intestinal lymphoma may be present in some dogs with CIE. Canine primary intestinal lymphoma, predominantly of T-cell origin, is treated with lomustine (CCNU)-based chemotherapy protocols; however, the median survival time is less than 62 days [12]. Lymphoplasmacytic enteritis, a common feature of CIE, can be difficult to distinguish from small cell intestinal lymphoma because of their similar clinical presentations and histopathologic findings [8,13]. Clonality testing using polymerase chain reaction for antigen receptor rearrangement and immunohistochemistry for CD3 and CD20 may improve diagnostic accuracy, but these methods are not always sensitive enough to detect canine intestinal lymphomas [13–15]. Therefore, the application of MSC-based therapy for CIE could potentially influence the progression of undiagnosed intestinal lymphomas.

Although the role of MSCs in hematologic malignancies such as lymphomas and leukemias is less completely understood than in solid tumors, human MSCs also appear to have dual effects on lymphoma/leukemia (LL) cells, either supporting or inhibiting their development by differentially affecting apoptosis and the cell cycle [16]. However, no studies have investigated the effects of canine MSCs on the development of hematologic malignancies in dogs; thus, the risk of MSC-based therapy promoting the progression of intestinal lymphoma in CIE remains unknown. Given this, the purpose of our study was to evaluate the safety of MSC-based therapy for CIE, focusing on its potential pro-tumorigenic characteristics. To this end, we investigated the effects of cADSCs on the proliferation, apoptosis, and cell cycle of various canine LL cell lines in vitro, as well as the growth of an intestinal lymphoma cell line derived from a dog in vivo.

2. Methods

2.1. Isolation, culture, and characterization of cADSCs

cADSCs were isolated from the falciform ligament fat aseptically collected under anesthesia from five healthy male beagle dogs (mean age, 2.2 years; mean weight, 10.5 kg), as previously described [17]. Dogs were premedicated with intravenous medetomidine (domitor 1 mg/mL; Zenoaq, Koriyama, Japan) 5 μg/kg body weight, then anesthesia was induced with intravenous propofol (propofol 10 mg/mL; Maruishi Pharmaceutical, Tokyo, Japan) 1–8 mg/kg body weight to effect, and maintained with isoflurane (ds isoflurane; DS Pharma, Osaka, Japan) mixed with oxygen. Postoperative analgesia of the dogs was performed by subcutaneous injection of 20 μg/kg body weight of buprenorphine (lepetan 0.2 mg/mL; Otsuka Pharmaceutical, Tokyo, Japan) every 8 h. The adipose tissue was digested in Dulbecco's Modified Eagle's Medium (DMEM) containing 1.5 % collagenase type I (Sigma-Aldrich, St. Louis, MO, USA) with gentle agitation at 37 °C for 1 h, followed by centrifugation at 700×*g* for 5 min to obtain cell pellets containing stromal vascular fractions. The pellets were resuspended in DMEM, filtered through a 100-μm nylon mesh, and centrifuged at 400×*g* for 5 min to remove residue in the supernatant. The pellets were then suspended in DMEM complete medium (DMEM supplemented with 10 % fetal bovine serum and 1 % penicillin–streptomycin), plated in T-75 culture flasks, and incubated overnight in a humidified atmosphere with 5 % CO_2 at 37 °C. The medium was changed every 2–3 days, and once 70 %–80 % confluence was reached, the cells were detached using trypsin-EDTA solution and passaged. All experiments used cADSCs at passages 2 to 3. As previously reported [17], cADSCs were confirmed for distinctive surface marker expression patterns (CD29, CD44, and CD90 positive; CD34, CD45, and HLA-DR negative) and tri-lineage differentiation potential (adipogenesis, osteogenesis, and chondrogenesis). Details of the antibodies used to identify cell surface markers of cADSCs are shown in Supplementary Table S1.

All animal experiments were approved by the Bioethics Committee of Nippon Veterinary and Life Science University (approval number 2021S-40; September 8, 2021 and 2024S-25; July 26, 2024). Animals were handled in accordance with the animal care guidelines of the Institute of Laboratory Animal Resources of Nippon Veterinary and Life Science University, which conform to national and international guidelines, including the ARRIVE guidelines.

2.2. Culture of canine LL cell lines

Six previously established canine LL cell lines were used in this study: CLC [18], CLK [18], and Ema [18] cells were kindly provided by Dr. Takuya Mizuno (Yamaguchi University, Japan), and CL-1 [19], UL-1 [18], and GL-1 [20] cells were kindly provided by Dr. Hirotaka Tomiyasu (University of Tokyo, Japan). CLC, CLK, Ema, and CL-1 cells were characterized as T-cell lymphoma (TCL), UL-1 as T-cell acute lymphoblastic leukemia (ALL), and GL-1 as a B-cell ALL phenotype [18–21]. All LL cell lines were cultured in RPMI complete medium (RPMI-1640 supplemented with 10 % fetal bovine serum, 1 % penicillin–streptomycin, and 50 μM 2-mercaptoethanol) in a humidified atmosphere with 5 % CO_2 at 37 °C. The cells were maintained by passaging every 2 days.

2.3. Proliferation inhibition assay of LL cell lines

cADSCs were thawed, suspended in DMEM complete medium, plated on 150-mm cell culture dishes, and incubated in 5 % CO_2 at 37 °C for 3 days. The cells were then detached and treated with 40 μg/mL mitomycin C (Nacalai Tesque, Kyoto, Japan) at 37 °C for 3 h with occasional agitation. After treatment, the cells were washed twice with phosphate-buffered saline (PBS), resuspended in DMEM complete medium, and plated directly into 96-well plates at densities of 1×10^3, 5×10^3, or 2×10^4 cells/well in 0.1 mL medium. Alternatively, they were plated at 5×10^3 cells/well in 0.1 mL medium on Transwell membranes (Corning Inc., Corning, NY, USA) and incubated overnight.

After incubation, the medium was removed, and CLC, CLK, Ema, CL-1, UL-1, and GL-1 cells were added either to the top of the wells with or without cADSCs, or to the bottom of the Transwell membranes with or without cADSCs, at a density of 5×10^3 cells/well in 0.1 mL RPMI complete medium. These cultures were then incubated in 5 % CO_2 at 37 °C for 24, 48, and 72 h. Wells without cells and those containing only mitomycin C-treated cADSCs were used as blanks and controls, respectively. After the incubation period, a Cell Counting Kit-8 reagent (Dojindo, Kumamoto, Japan) was added to each well and incubated for an additional 2 h.

The number of viable cells at each time point was measured by the optical density (OD) at 450 nm using a Synergy HT Microplate Reader (BioTek, Winooski, VT, USA). The OD_{450} values were calculated as follows: OD_{450} of LL cells with cADSCs minus OD_{450} of cADSCs alone. Cell proliferation was determined by calculating the fold change in OD_{450} at each time point relative to the OD_{450} after 24 h of co-culture.

2.4. Apoptosis assay of LL cell lines

cADSCs were plated into six-well plates or onto Transwell membranes at a density of 2×10^5 cells/well in DMEM complete medium and incubated overnight to allow for cell attachment. The medium was then removed, and LL cells were added at 2×10^5 cells/well in 3 mL of RPMI complete medium, either directly to the wells with or without cADSCs or to the bottom of the membranes with cADSCs, and cultured. After 72 h, the floating LL cells were separated from the cADSCs by gentle pipetting or by removing the membrane. The LL cells were then collected and stained using an FITC Annexin-V Apoptosis Detection Kit with propidium iodide (PI) (BioLegend, San Diego, CA, USA), following the manufacturer's instructions.

Apoptotic cells were measured by flow cytometry, identifying cells positive for Annexin V alone or in combination with PI. Flow cytometry was performed using a CytoFLEX instrument (Beckman Coulter, Brea, CA, USA), and data were analyzed using CytExpert version 2.0 software.

2.5. Cell cycle distribution analysis of LL cell lines

As in the apoptosis assay, cADSCs and LL cells were co-cultured at a 1:1 ratio in six-well plates, either directly or indirectly using Transwell inserts, for 72 h. Afterward, the floating LL cells were collected. The LL cells were then stained using a Cell Cycle Assay Solution Deep Red (Dojindo) according to the manufacturer's instructions. The percentage of cells in the G0/G1, S, and G2/M phases of the cell cycle was determined by flow cytometry.

2.6. Transduction of firefly luciferase gene into CLC lymphoma cells

Lentiviral vectors were used to transduce the firefly luciferase (*fLuc*) gene into CLC cells using the pLV[Exp]-Neo-CMV > Luciferase vector, which was constructed and packaged by VectorBuilder (Chicago, IL, USA). The vector ID VB90088-2567cxn can be used to retrieve detailed information about the vectors on vectorbuilder.com. CLC cells were plated in six-well plates and infected in 2 mL RPMI with 8 μg/mL polybrene (VectorBuilder) and lentivirus at a multiplicity of infection of 10 for 24 h. The cells were then washed twice with PBS, resuspended in 3 mL of RPMI complete medium, and plated in six-well plates. They were incubated in 5 % CO_2 at 37 °C.

After 48 h, the cells were suspended in RPMI complete medium supplemented with 1 mg/mL G-418 (Promega, Madison, WI, USA) for clonal selection and cultured for 10 days, with the medium changed every 2 days. Following clonal selection, CLC/*fLuc* cells were plated in 24-well plates at concentrations ranging from 1×10^4 to 1×10^7 cells/well in 1 mL PBS. Bioluminescence was captured using a Fusion FX7 imaging system (Vilber, Marne-la-Valée, France) immediately after adding 10 μL of D-luciferin (30 mg/mL; Abcam, Cambridge, UK) to each well to confirm *fLuc* expression. The bioluminescence and image data were analyzed using Kuant version 2.4 software (Vilber), and the CLC/*fLuc* clones with the highest luciferase activity were selected for subsequent experiments.

2.7. Bioluminescent canine lymphoma cell xenotransplantation and cADSC treatment in immunocompromised mice

Twenty-four 6-week-old male SCID/Beige mice were purchased from Jackson Laboratory Japan (Kanagawa, Japan), housed and handled aseptically in autoclaved isolator cages with temperature and light control, and provided ad libitum access to sterile water and food. The xenotransplantation model of bioluminescent canine lymphoma cells was established by subcutaneous injection of 1×10^5 CLC/*fLuc* cells suspended in 100 μL of PBS into the lumbar region of the mice. The mice were divided into four groups according to the number of cADSCs co-injected with CLC/*fLuc* cells as follows ($n = 6$/group):

- Control group: injected with 100 μL of PBS without cADSCs
- Low-dose group: injected with 2×10^4 cADSCs (CLC/*fLuc*: cADSC = 1:0.2)
- Equal-dose group: injected with 1×10^5 cADSCs (CLC/*fLuc*: cADSC = 1:1)

- High-dose group: injected with 1×10^6 cADSCs (CLC/*fLuc*: cADSC = 1:10)

Injections of cADSCs without CLC/*fLuc* cells were repeated on days 7 and 14 at the indicated doses. The mice underwent bioluminescence imaging on days 0, 7, 14, and 21. The mice were sacrificed on day 22, and the subcutaneous tumor masses were harvested for weight measurement while the lungs were collected for ex vivo bioluminescence imaging.

2.8. Bioluminescence imaging

Mice inoculated with CLC/*fLuc* cells, with or without cADSC treatment, were anesthetized using a three-anesthetic mixture of medetomidine, midazolam, and butorphanol followed by an intraperitoneal injection of 150 mg/kg D-luciferin. The mice were placed in the imaging chamber, and 20 min after D-luciferin injection, they were imaged in the prone position with a 2-min exposure time using a Fusion FX7 imaging system.

For ex vivo bioluminescence imaging of the lungs, the anesthetized mice were euthanized by exsanguination through cardiac blood collection 2 min after D-luciferin injection, and their lungs were quickly harvested. The harvested lungs were soaked in 500 μL of D-luciferin (0.3 mg/mL) and immediately imaged with a 2-min exposure time. Bioluminescence data from all mice and lung samples at each time point were analyzed using Kuant software. The bioluminescence intensity was quantified by setting the region of interest on the image where the bioluminescence signal was overlaid.

2.9. Histological examination

Tumor mass samples from the mice were fixed in 10 % neutral-buffered formalin for 24 h after weight measurement. The samples were then transferred to 100 % ethanol, embedded in paraffin, sectioned into 3-μm slices, and stained with hematoxylin and eosin. Histological evaluations of the sections were performed by two pathologists.

2.10. Statistical analysis

All data are presented as the mean ± standard deviation. The normality of the data was tested using the Shapiro–Wilks normality test. For differences between multiple groups, normally distributed data were analyzed with one-way analysis of variance and compared using Dunnett's test or the Tukey–Kramer multiple comparison post hoc test. Non-normally distributed data were analyzed with the Kruskal–Wallis test and compared using the Steel–Dwass post hoc test. A p-value of <0.05 was considered statistically significant. Statistical analyses were performed using R Commander 4.1.2.

3. Results

3.1. cADSCs inhibit the proliferation of canine LL cell lines via cell-to-cell contact in vitro

We first investigated the effect of cADSCs on the proliferation of canine hematologic malignancy cells in vitro. For this purpose, CLC, CLK, Ema, and CL-1 (TCL) cells; UL-1 (T-ALL) cells; and GL-1 (B-ALL) cells were co-cultured directly with cADSCs at ratios of 0.2, 1, or 5 cADSCs per LL cell for 72 h cADSCs exhibited a proliferation-inhibitory effect on LL cells across all lineages, with the effect becoming stronger as both the number of cADSCs and the co-culture time increased (Fig. 1a). By contrast, when LL cell lines were co-cultured with cADSCs without direct cell-to-cell contact using Transwell inserts (which allow diffusion of soluble factors but prevent physical contact), proliferation was not inhibited in any LL cell line and was instead promoted in Ema cells (Fig. 1b).

3.2. cADSCs differentially affect survival and cell cycle of different LL cell lines in vitro

Previous studies have shown that the effects of human and mouse MSCs on the proliferation of hematologic malignancy cells are mediated through the regulation of tumor cell apoptosis and the cell cycle [15]. To explore the mechanisms by which cADSCs influence canine LL cell proliferation, we investigated the apoptosis and cell cycle of LL cells co-cultured with or without cADSCs. Apoptosis was measured by flow cytometry as the frequency of cells positive for Annexin V and/or PI. Compared to LL cells cultured alone, direct co-culture with cADSCs at a 1:1 ratio for 72 h significantly induced apoptosis in the TCL cell lines CLC, CLK, Ema, and CL-1. However, apoptosis was not induced in the T-ALL cell line UL-1, and apoptosis was suppressed rather than induced in the B-ALL cell line GL-1 (Fig. 2a–f).

By contrast, when cADSCs and LL cells were separated using a Transwell system, apoptosis was only induced in CLC cells, and the pro-apoptotic or anti-apoptotic effects of cADSCs were lost in the other LL cell lines (Fig. 2a–f).

To further investigate, LL cells were co-cultured with or without cADSCs at a 1:1 ratio for 72 h, and their cell cycle distribution was analyzed. Ema, CL-1, UL-1, and GL-1 showed an increased proportion of cells in the G0/G1 phase and a decreased proportion in the G2/M phase after co-culture with cADSCs compared with monoculture. By contrast, CLC and CLK showed no significant changes in the proportions of cells in each phase (Fig. 3a–f). When cADSCs and LL cells were co-cultured with physical separation, CLC exhibited a decrease in G0/G1 phase cells and an increase in G2/M phase cells, while Ema showed a decrease in G0/G1 phase cells and an increase in S and G2/M phase cells. However, the other cell lines showed no significant changes (Fig. 3a–f).

A summary of these in vitro experiment results is provided in Table 1.

3.3. Establishment of bioluminescent canine lymphoma cell line with transduction of fLuc gene

We next examined the effect of cADSCs on the growth of canine lymphoma cell lines in vivo. Because the goal of this study was to investigate the effect of cADSCs on potential intestinal lymphoma in dogs with CIE, we used CLC lymphoma cells, which were previously isolated from a dog with a clinical diagnosis of gastrointestinal lymphoma with cytology of abdominal lymph node and have been reported to have the highest proliferative capacity both in vitro and in immunocompromised mice [18]. The *fLuc* gene was transduced by infecting CLC cells with a lentiviral vector to establish the bioluminescent canine lymphoma cell line CLC/*fLuc*, which allows for tracking tumor growth in vivo. No morphological differences were observed between the naive CLC cells and the transduced CLC/*fLuc* cells (Fig. 4a). The bioluminescence intensity was directly proportional to the number of viable CLC/*fLuc* cells, confirming that higher detected luminescence indicates a greater number of tumor cells (Fig. 4b).

3.4. cADSCs inhibit canine lymphoma cell growth in xenotransplantation mouse models in a dose-dependent manner

To investigate the direct effect of cADSCs on the in vivo growth of canine lymphoma cells, CLC/*fLuc* cells were co-injected subcutaneously with different numbers of cADSCs into SCID/Beige mice,

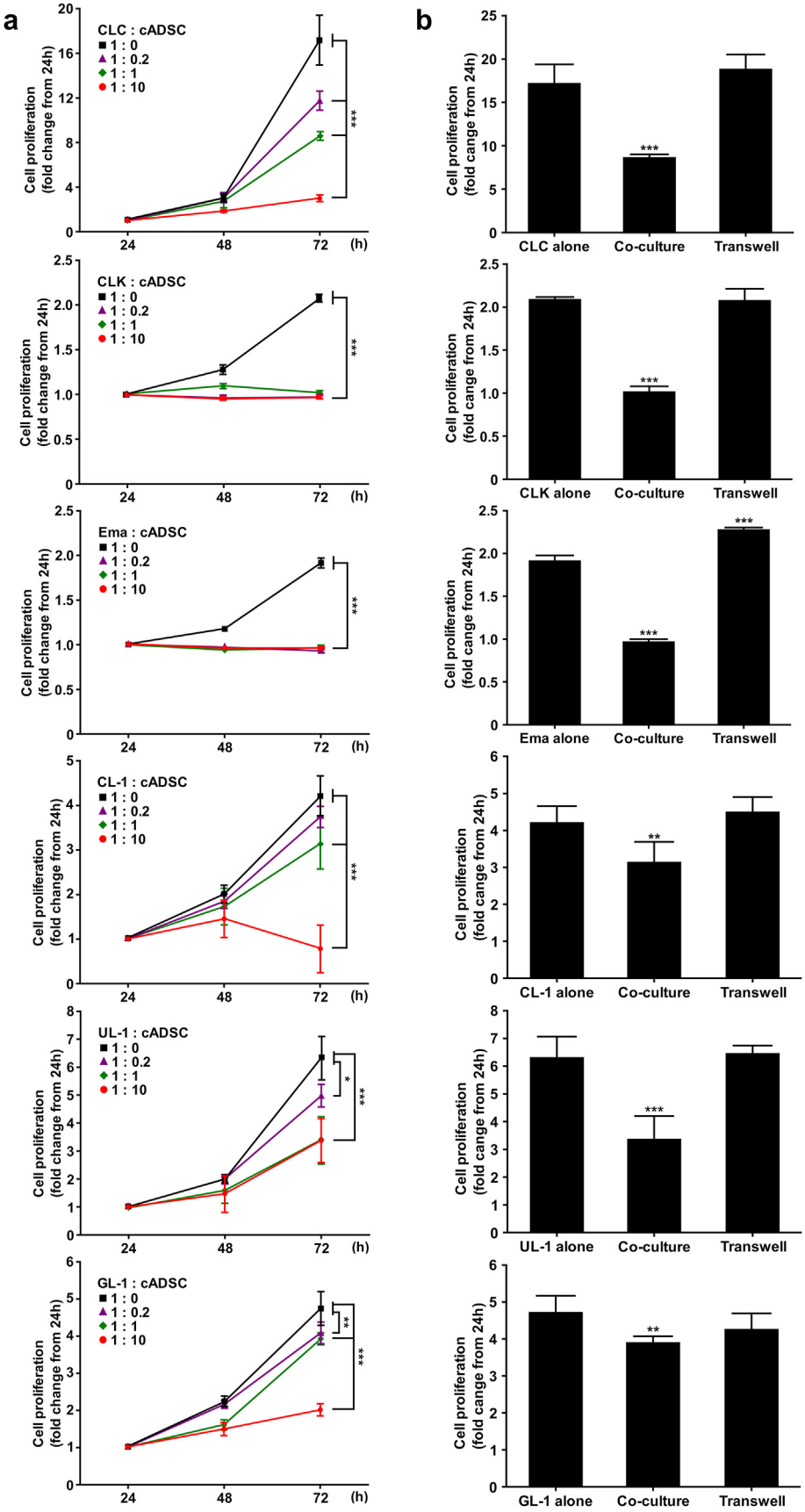

Fig. 1. Inhibitory effect of canine adipose-derived mesenchymal stromal cells (cADSCs) on the proliferation of hematologic malignancy cells in vitro. (a) Proliferation of six different lineages of leukemia/lymphoma cells cultured alone or co-cultured with varying numbers of cADSCs (ratios of 0.2:1, 1:1, and 10:1). Cell proliferation after 48 and 72 h was measured spectrophotometrically as optical density and presented as a fold change from the optical density value at 24 h. (b) Proliferation of 5×10^3 leukemia/lymphoma cells cultured alone or co-cultured with 5×10^3 cADSCs, either directly or indirectly (Transwell inserts), for 72 h. Data are expressed as the mean ± standard deviation from experiments performed in triplicate ($n = 3$). *$p < 0.05$, **$p < 0.01$, ***$p < 0.001$ vs. LL cells cultured alone.

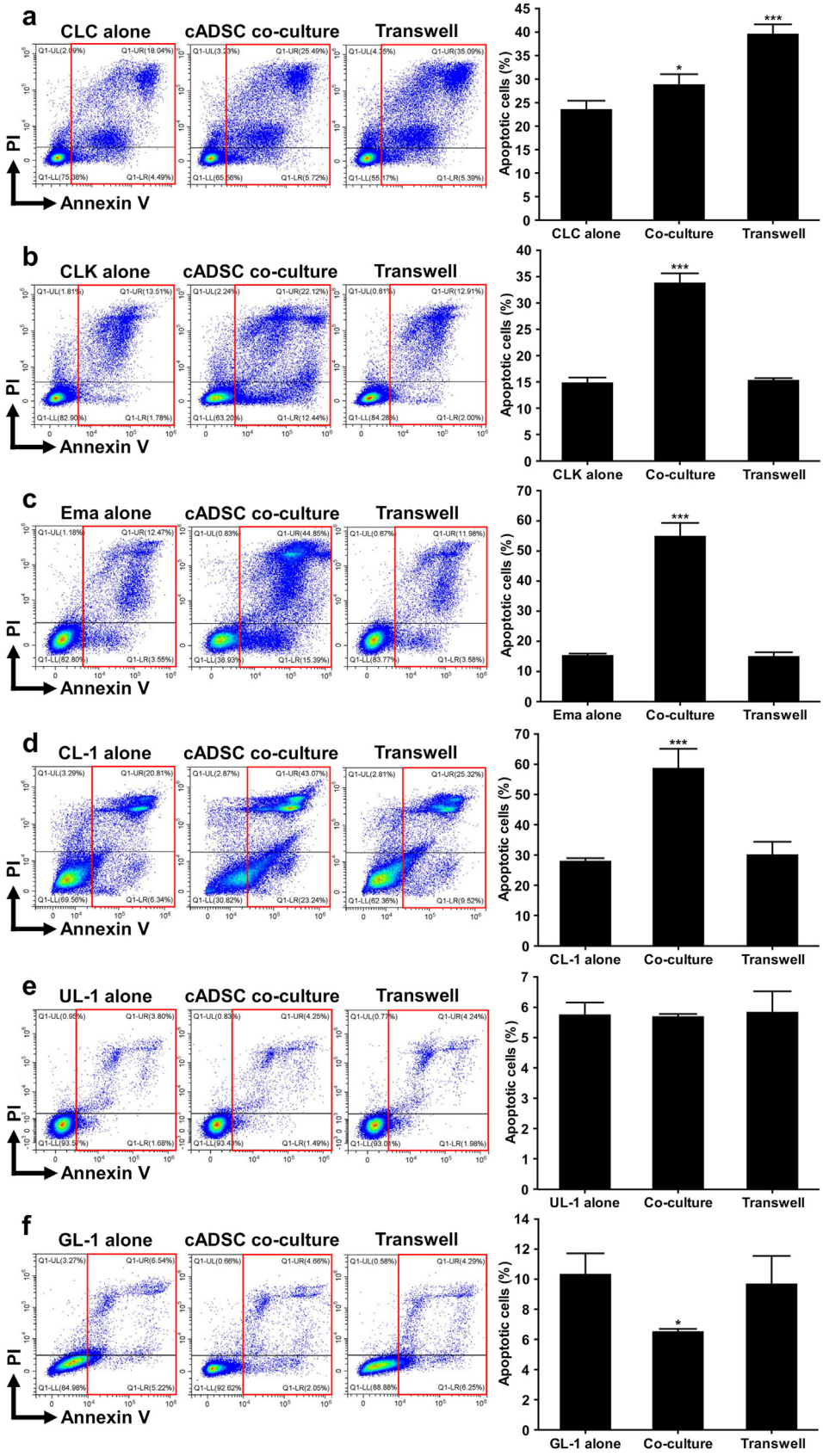

Fig. 2. Differential effects of canine adipose-derived mesenchymal stromal cells (cADSCs) on leukemia/lymphoma (LL) cell survival. LL cells were cultured alone or co-cultured directly or indirectly with cADSCs at a 1:1 ratio for 72 h, followed by flow cytometry to assess the frequency of Annexin V and/or propidium iodide (PI)-positive apoptotic cells. Representative dot plots and the frequency of apoptotic cells under different culture conditions are shown for (a) CLC, (b) CLK, (c) Ema, (d) CL-1, (e) UL-1, and (f) GL-1. Red boxes indicate Annexin V and/or PI-positive apoptotic cells. Data are expressed as the mean ± standard deviation from experiments performed in triplicate ($n = 3$). *$p < 0.05$, ***$p < 0.001$ vs. LL cells cultured alone.

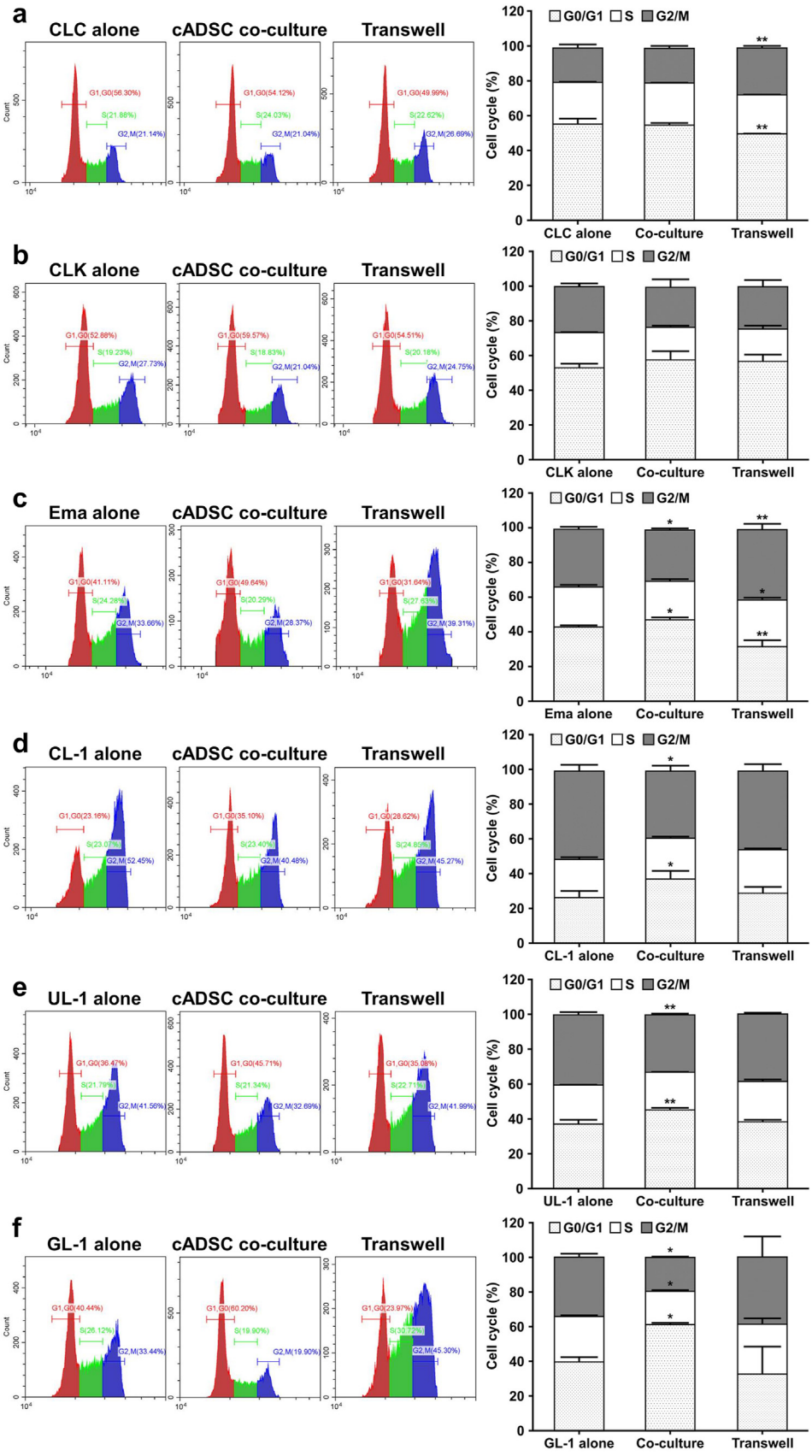

Fig. 3. Differential effects of canine adipose-derived mesenchymal stromal cells (cADSCs) on the cell cycle of leukemia/lymphoma (LL) cells. LL cells were cultured alone or co-cultured with cADSCs at a 1:1 ratio for 72 h, after which they were collected and subjected to cell cycle distribution analysis by flow cytometry. Representative histograms and the proportions of cells in the G0/G1, S, and G2/M phases under different culture conditions are shown for (a) CLC, (b) CLK, (c) Ema, (d) CL-1, (e) UL-1, and (f) GL-1. Data are expressed as the mean ± standard deviation from experiments performed in triplicate ($n = 3$). *$p < 0.05$, **$p < 0.01$ vs. LL cells cultured alone.

Table 1
Summary of in vitro experiments.

	Direct co-culture			Transwell		
	Proliferation	Apoptosis	Cell cycle	Proliferation	Apoptosis	Cell cycle
CLC	Inhibited	Induced	No effect	No effect	Induced	G2/M increased
CLK	Inhibited	Induced	No effect	No effect	No effect	No effect
Ema	Inhibited	Induced	G0/G1 arrested	No effect	No effect	G2/M and S increased
CL-1	Inhibited	Induced	G0/G1 arrested	No effect	No effect	No effect
UL-1	Inhibited	No effect	G0/G1 arrested	No effect	No effect	No effect
GL-1	Inhibited	Suppressed	G0/G1 arrested	No effect	No effect	No effect

which are characterized by dysfunction in T and B lymphocytes as well as natural killer cells. The mice received weekly injections of the same dose of cADSCs as the initial injection, and lymphoma cell growth was monitored over time using weekly bioluminescence imaging until the mice were sacrificed on day 22.

Bioluminescence signals were detected in all mice injected with CLC/*fLuc* cells, regardless of whether cADSCs were co-injected, and the intensity increased over time (Fig. 5a). However, mice co-injected with higher doses of cADSCs exhibited lower bioluminescence intensity at each time point than those co-injected with lower doses or no cADSCs (Fig. 5b). By day 21, mice co-injected with any dose of cADSCs did not show higher bioluminescence intensity than those without cADSCs (Fig. 5c). Consistent with the bioluminescence imaging results, the tumor mass weight removed from the sacrificed mice was similar between the low-dose group (CLC/*fLuc*:cADSC = 1:0.2) and the control group (CLC/*fLuc*:cADSC = 1:0), but significantly lower in the equal-dose (CLC/*fLuc*:cADSC = 1:1) and high-dose (CLC/*fLuc*:cADSC = 1:10) groups (Fig. 5d and e).

Histopathologic examination revealed that the tumors formed in the xenografts had a similar histology across all groups (Fig. 5f). The tumors were characterized by a diffuse proliferation of large cells with round to irregular nuclei, prominent nucleoli, and a small amount of amphophilic cytoplasm, with frequent mitotic figures.

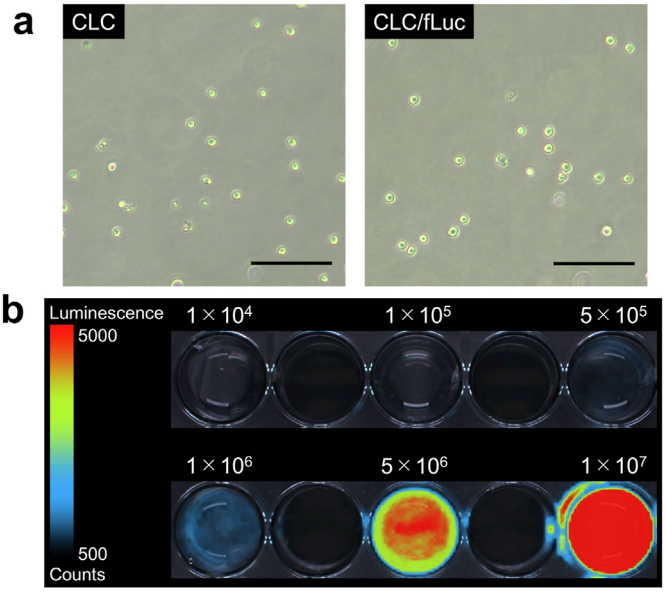

Fig. 4. Establishment of firefly luciferase (*fLuc*)-expressing canine lymphoma cell line. (a) Microscopic morphology of naïve CLC cells (left panel) and CLC/*fLuc* cells transduced with lentiviral vectors (right panel). Scale bar = 100 μm. (b) Luciferase activity of CLC/*fLuc* cells plated at graded cell numbers from 10^4 to 10^7, evaluated by detecting bioluminescence using the Fusion FX7 imaging system. The bioluminescence signal is depicted as pseudocolor (red = intense, blue = less intense), and the color scale indicates luminescence intensity per pixel.

This indicated that the tumors were primarily composed of lymphoma cells rather than spindle-shaped stromal cells. Necrosis was observed more frequently in the control and low-dose groups, which had larger tumor masses, suggesting that the necrosis was due to increased intracapsular pressure from tumor growth rather than a pro-apoptotic effect of cADSCs.

These data suggest that cADSCs inhibit, rather than promote, the growth of canine lymphoma cells in immunocompromised mice.

3.5. cADSCs delay the development of canine lymphoma cell metastasis

While it has been reported that human MSCs promote breast cancer cell metastasis by secreting chemokine ligand type 5 [22], they have also been shown to inhibit breast cancer cell growth and metastasis by blocking the phosphoinositide 3-kinase/protein kinase B signaling pathway [23]. Given these conflicting effects of MSCs on metastatic development and tumor cell growth, we investigated the effects of cADSCs on the metastasis of canine lymphoma cells in our xenotransplantation model.

As shown in Fig. 6a, a representative ex vivo bioluminescence image of major organs from a sacrificed xenotransplantation mouse, bioluminescence signals indicating the presence of CLC/*fLuc* cells were detected only in the lungs of all mice. Mice without cADSC treatment and those treated with low doses of cADSCs exhibited comparably high lung bioluminescence intensity, while the intensity was lower in mice treated with higher doses of cADSCs. Notably, in two mice treated with high doses of cADSCs (2/6, 33 %), no bioluminescence signal was detected in the lungs (Fig. 6b and c). These findings indicate that cADSCs dose-dependently inhibited the development of canine lymphoma cell metastasis in immunocompromised mice.

4. Discussion

We investigated the effect of cADSCs on the proliferation of canine LL cells of different lineages to assess the safety of MSC-based therapy in terms of tumor development. Our results demonstrated that cADSCs inhibited the proliferation of all canine LL cell lineages in vitro through cell-to-cell contact in a time- and dose-dependent manner. To the best of our knowledge, this is the first study to report the inhibitory effect of cADSCs on the proliferation of canine LL cell lines.

However, conflicting effects of human MSCs on the proliferation of hematologic malignancy cells in vitro have been reported, with studies showing either inhibitory or promotional effects. Tian et al. [24] reported that human umbilical cord-derived MSCs (UCMSCs) markedly inhibited proliferation of the acute promyelocytic leukemia cell line HL-60 and the chronic myelogenous leukemia cell line K562 in vitro by arresting the cell cycle in the G0/G1 phase through phosphorylation of p38 mitogen-activated protein kinase. Similarly, Yuan et al. [25] reported that human UCMSCs induced G0/G1 phase arrest and inhibited proliferation of the T-ALL cell line

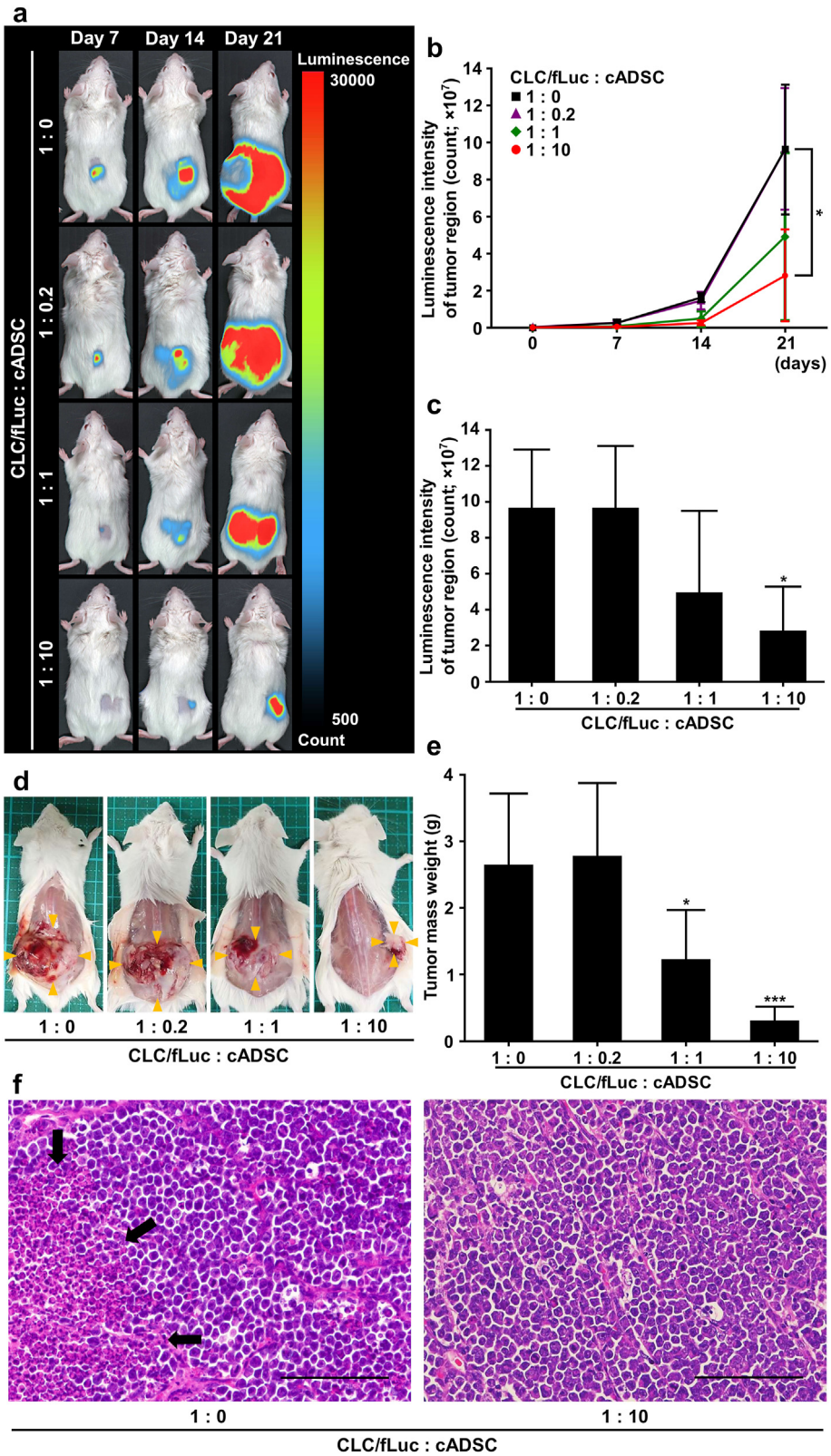

Fig. 5. Growth inhibitory effect of canine adipose-derived mesenchymal stromal cells (cADSCs) on canine bioluminescent lymphoma cells in xenotransplantation mouse models. (a) Representative bioluminescence images on days 7, 14, and 21 showing tumor growth in CLC/*fLuc* cell xenotransplantation mouse models treated with different doses of cADSCs. (b) Changes in mean luminescence intensity in the tumor region from day 0 to day 21 in xenotransplantation mouse models treated with different doses of cADSCs. (c) Comparison of mean luminescence intensity in the tumor region on day 21 in mice treated with different doses of cADSCs. (d) Macroscopic images of tumor masses (yellow arrowhead) in xenotransplantation mouse models treated with different doses of cADSCs and sacrificed on day 22. (e) Comparison of mean tumor mass weight on day 22 in xenotransplantation mouse models treated with different doses of cADSCs. (f) Histological images of tumor masses in xenotransplantation mouse models treated with high-dose cADSCs (right panel) or without cADSC treatment (left panel). Black arrows indicate necrotic nests in the inner layer of the tumor mass. Scale bar = 100 μm. Data are expressed as the mean ± standard deviation ($n = 6$). *$p < 0.05$, ***$p < 0.001$ vs. control group (CLC/*fLuc*:cADSC = 1:0).

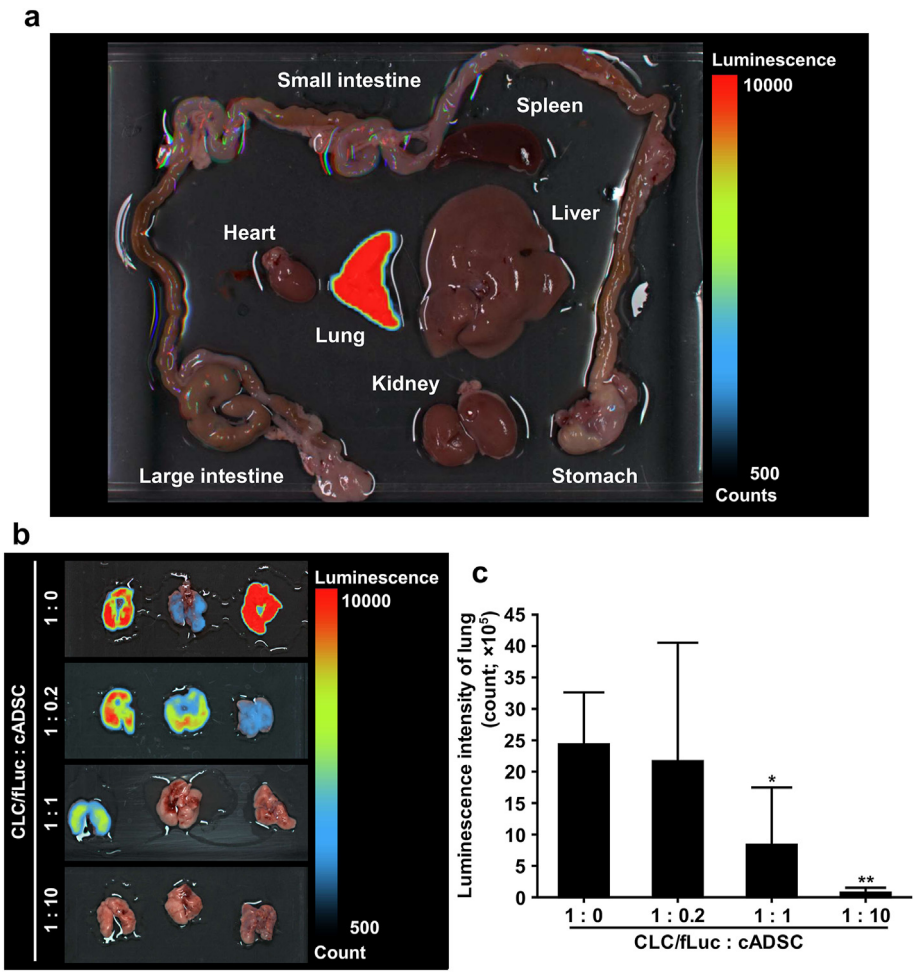

Fig. 6. Inhibitory effect of canine adipose-derived mesenchymal stromal cells (cADSCs) on metastatic development of canine bioluminescent lymphoma cells. (a) Representative ex vivo bioluminescence image of major organs from a sacrificed xenotransplantation mouse model. (b) Bioluminescence images of lungs taken from xenotransplantation mouse models treated with different doses of cADSCs. (c) Comparison of mean luminescence intensity in the lungs on day 22 in mice treated with different doses of cADSCs. Data are expressed as the mean ± standard deviation ($n = 6$). *$p < 0.05$, **$p < 0.01$ vs. control group (CLC/*fLuc*:cADSC = 1:0).

Jurkat. By contrast, Panayiotidis et al. [26] showed that human bone marrow-derived MSCs (BMSCs) protected tumor cells derived from patients with B-chronic lymphocytic leukemia from apoptosis via direct adhesion, thereby prolonging cell survival. Likewise, Nwabo Kamdje et al. [27] demonstrated that human BMSCs exert anti-apoptotic effects on leukemic cells from patients with B-ALL, mediated by the activation of Notch signaling through cell-to-cell contact.

As in these studies, most reports of the anti-tumorigenic effects of MSCs involve immortalized LL cell lines, while studies reporting pro-tumorigenic effects have typically used primary LL cells derived from patients [16]. Immortalized cell lines may harbor significant mutations that alter primary cell traits, which has also been suggested for the cell lines used in this study [18,21,28,29]. These differences in cell traits may contribute to the conflicting effects of MSCs on tumor cell proliferation. Therefore, similar studies using primary canine LL cells are needed to ensure the safety of MSC-based therapies in veterinary medicine.

Multiple mechanisms have been proposed by which human MSCs inhibit the proliferation of hematologic malignancy cells in vitro. The most widely accepted of these mechanisms is that MSCs induce cell cycle arrest in tumor cells. Liang et al. [30] showed that a human bone marrow fibroblastoid stromal cell line induces G0/G1 phase arrest and inhibits cell proliferation by regulating the expression of specific cell cycle-related genes in HL-60 cells. Similarly, Sarmadi et al. [31] demonstrated that human BMSCs inhibit cell proliferation by arresting the cell cycle of Jurkat cells and the B-cell progenitor leukemia cell line BV173 at the G0/G1 phase via intercellular contact. Additionally, it has been reported that human MSCs can induce tumor cell death. For example, Ahn et al. [32] reported that co-culture of human ADSCs with the mouse TCL cell line EL4 induces apoptosis by activating caspase-3 and causing cleavage of poly ADP-ribose polymerase in EL4 cells.

Consistent with these reports, our results demonstrate that cADSCs inhibit canine LL cell proliferation in vitro by modulating cell survival and/or the cell cycle. However, cADSCs had different effects on the survival and cell cycle of various cell lines. Specifically, cell proliferation was inhibited in CLC and CLK cells through the induction of cell death, in UL-1 and GL-1 cells through the induction of G0/G1 phase arrest, and in Ema and CL-1 cells through both mechanisms.

Previous studies have revealed differences in cell cycle-related gene and protein expression, as well as epigenetic changes, in different canine LL cell lines. For the cell lines used in this study, research has shown decreased expression of the endogenous cyclin-dependent kinase (CDK) inhibitor p16 protein and hyperphosphorylation of retinoblastoma protein (pRb) due to *p16* gene hypermethylation in CLC and UL-1 cells [33], decreased expression

of p16 protein and hyperphosphorylation of pRb due to abnormal *p16* gene (including deletion) in Ema cells [33], high expression of the *p16* gene and protein in GL-1 cells [33], possible deletion of pRb in CL-1 cells [34], and possible deletion of pRb or downstream bypass in UL-1 cells [35]. These differences in the regulatory mechanisms of the cell cycle among cell lines have been shown to affect their sensitivity to various inhibitors, such as the pan-CDK inhibitor flavopiridol [34], the CDK4/6 inhibitors palbociclib and abemaciclib [35], and the hydroxymethylglutaryl-coenzyme A reductase inhibitor simvastatin [36] for inducing cell cycle arrest and cell death. The differential effects of cADSCs on these LL cell lines may also be related to these variants, but the molecular mechanisms underlying the actions of cADSCs remain unclear in this study. Further investigation is needed to elucidate the mechanisms by which cADSCs inhibit the proliferation of canine lymphoma cells in more detail.

To determine whether the proliferation-inhibitory effect of cADSCs on the canine LL cell lines was dependent on cell-to-cell contact, both cell types were also co-cultured under physical separation using Transwell membranes. When separated from cADSCs, cell death in CLC cells increased compared to conditions with intercellular contact, while the proportion of cells in the G2/M phase increased, and the proliferation-inhibitory effect of cADSCs was lost. In Ema cells, separation from cADSCs led to a loss of apoptosis induction, an increase in cells in the S- and G2/M phases, and a reversal of the cADSC proliferation-inhibitory effect to a promoting effect. The fact that proliferation recovered or was promoted after separation from cADSCs suggests that the increase in S-phase or G2/M-phase cells was not due to cell cycle arrest at these stages, but rather an accelerated progression from the G1 to S phase.

In other LL cell lines, isolation from cADSCs resulted in the loss of cell death induction or cell cycle arrest, leading to recovered proliferation. Similar observations have been reported in a study using mouse cells. Song et al. [37] found that co-culture of mouse BMSCs without cell-to-cell contact did not inhibit the proliferation of the mouse B-cell lymphoma (BCL) cell line A20, whereas co-culture with cell-to-cell contact inhibited A20 cell proliferation by inducing cell cycle arrest and apoptosis while also inhibiting IL-10 secretion from tumor cells. By contrast, Ahn et al. [32] showed that human ADSCs inhibited the proliferation of the mouse TCL cell line EL4 with or without cell-to-cell contact, and Li et al. [38] reported that human UCMSCs promoted the proliferation of the human BCL cell line Raji in a contact-dependent manner.

Although discrepancies exist between studies, likely due to differences in MSC sources (e.g., species or tissue of origin) or the types of LL cell lines used, our results suggest that the inhibition of canine lymphoma cell proliferation by cADSCs is mediated by cell-to-cell contact or contact-induced secreted factors. However, a key finding of this study, which raises concerns about the safety of MSC-based therapy, is that cADSCs promoted Ema cell proliferation through secreted factors. Further studies are needed to analyze cell cycle-related genes and proteins in Ema cells exposed to the cADSC secretome, as well as to identify the specific secreted factors that may affect them.

Some studies have reported differing effects of human MSCs on tumor cell growth in vitro and in vivo. Ramasamy et al. [39] demonstrated that human BMSCs inhibit BV173 cell proliferation in vitro by inducing G0/G1 phase arrest and decreasing cyclin D2 expression, yet they promote tumor growth in vivo by protecting against apoptosis. Similarly, Tian et al. [40] reported that human BMSCs inhibit the growth of the human lung cancer cell line A549 and the human esophageal cancer cell line Eca-109 in vitro by inducing G0/G1 phase arrest and apoptosis, but they support tumor formation in nude mice by promoting tumor vascularization.

Given these findings, we also investigated the effect of cADSCs on the growth of a canine lymphoma cell line in vivo. Our results showed that cADSCs inhibited the growth of CLC lymphoma cells in a dose-dependent manner. Although few reports have elucidated mechanisms by which MSCs inhibit tumor growth in vivo, Zhu et al. [41] demonstrated that dickkopf-1 secreted by human ADSCs inhibits K562 cell growth by blocking the Wnt signaling pathway. Additionally, Secchiero et al. [42] suggested that human BMSCs inhibit tumor angiogenesis by inducing endothelial cell apoptosis, thereby suppressing the growth of the human BCL cell line BJAB in vivo. Although the exact mechanism by which cADSCs inhibited tumor growth in vivo remains unclear, direct inhibitory effects on tumor cells and tumor angiogenesis may have contributed.

However, it is important to consider that MSCs may indirectly promote or inhibit tumor growth by affecting the immunogenicity of tumor cells and the antitumor immunity of tumor-bearing animals because of their immunomodulatory properties that regulate immune cells involved in both innate and adaptive immunity [43]. In this regard, Lee et al. [44] reported that while human BMSCs inhibited A20 cell proliferation in vitro by inducing apoptosis, co-injection of both cell types into the lacrimal glands of immunocompetent BALB/c mice promoted tumor growth by creating an immunosuppressive microenvironment, characterized by increased regulatory T cells and myeloid-derived suppressor cells. Conversely, Lu et al. [45] showed that co-injection of mouse BMSCs and the mouse hepatocellular carcinoma cell line H22 into the abdominal cavity of BALB/c mice inhibited tumor progression without causing immunosuppression. Lin et al. [46] also suggested that the secretome of human Wharton's jelly-derived MSCs cultured under hypoxic conditions induces immunogenic cell death of tumor cells by increasing the expression of damage-associated molecular patterns and decreasing the expression of immune checkpoint molecules in the BCL cell line Ramos.

MSCs have conflicting effects on tumor cell growth as well as metastasis, and different studies have reported that MSCs promote or inhibit metastasis, even in tumor cell lines of the same lineage [22,23]. Mechanisms by which MSCs promote metastasis of solid tumors include transition of MSCs to tumor-associated fibroblasts [47] and promotion of epithelial-mesenchymal transition of tumor cells via transforming growth factor-β (TGF-β) [48], degradation and remodeling of extracellular matrix via matrix metalloproteinase [49], and signaling to tumor cells via secreted factors such as chemokine receptor (CCR) 5 ligand [4] and IL-17B [50]. In contrast, some studies have reported that MSCs inhibit the migration and invasion of breast cancer cells via secretion of tissue inhibitors of metalloproteinase (TIMP)-1 and -2 [51], and colorectal cancer cells via exosome-derived microRNA-4461 [52]. Li et al. [53] reported that MSCs inhibit metastasis in a hepatocellular carcinoma model by downregulating TGF-β expression in tumor cells. However, little is known about the effect of exogenously injected MSCs on the metastasis of hematologic malignancies.

This study showed that cADSCs inhibit lung metastasis in a dose-dependent manner in a CLC lymphoma model. This dose-dependent inhibitory effect was paralleled by local growth and lung metastasis, and thus the delay in lung metastasis may simply be the result of inhibition of CLC lymphoma cell growth. However, Li et al. [53] reported that secreted factors from human BMSCs promote local growth of the hepatocellular carcinoma cell line MHCC97-H cells while inhibiting lung metastasis, suggesting that the mechanisms underlying the effects of MSCs on local growth and distant metastasis of tumor cells may be different.

Hypoxia-inducible factor (HIF)-1α and CCR7 have been reported to contribute to the migration, invasion and metastasis of CLC lymphoma cell lines. HIF-1α is upregulated in L-CI.5s T lymphoma cells by elevated TIMP-1 levels in the tumor microenvironment and

promotes metastasis by inducing hepatocyte growth factor signaling [54]. Yamazaki et al. showed that nuclear HIF-1α protein is upregulated in CLC cells under hypoxic conditions [55]. Then, the same group demonstrated that the hypoxia-activated prodrug, evofosfamide, inhibits tumor growth and lung metastasis in a mouse model with a metabolic pathway very similar to that of dogs with gastrointestinal lymphoma by suppressing the expression of HIF-1α protein in CLC under hypoxic conditions [56]. In addition, Kanei et al. [57] evaluated CCR7 expression on CLC and UL-1 cells using Canine CCL19-human IgG-Fc fusion protein and found positive expression on CLC cells and negative expression on UL-1 cells. In a previous study [18], CLC cells showed a high rate of regional lymph node metastasis when injected intraperitoneally into immunocompromised mice, but UL-1 cells did not, suggesting the implication of CCR7 in regional lymph node metastasis. Therefore, investigating the interaction between cADSCs and CLC lymphoma cells, focusing on mediators such as TGF-β, TIMP, HIF-1α, and CCR7, is important to understand the mechanisms by which cADSCs inhibit lymphoma metastasis.

As in many previous studies [5,7,22,32,39–42,48–50,53], this study used immunocompromised mice to investigate the direct effects of cADSCs on canine lymphoma cell growth and metastasis under xenotransplantation conditions. Therefore, the effect of cADSCs on LL cell proliferation and migration should be further evaluated in immunocompetent animals in the future, also taking into account their impact on antitumor immunity.

5. Conclusions

Our results show for the first time that cADSCs inhibit the growth of canine LL cell lines both in vitro and in vivo. This study suggests that cADSC-based cell therapy could potentially be applied to CIE without promoting the development of intestinal lymphomas. However, to ensure the safety of cADSC-based therapies, further studies are needed to investigate their effects on primary tumor cell growth, explore the molecular mechanisms underlying LL cell growth and metastasis inhibition, and assess their impact on antitumor immunity in immunocompetent models.

Data availability

The original contributions presented in the study are included in the article. Further inquiries can be directed to the corresponding author.

Ethics statement

The animal study protocol was approved by the Bioethics Committee of Nippon Veterinary and Life Science University (approval number 2021S-40; September 8, 2021 and 2024S-25; July 26, 2024). Animals were handled in accordance with the animal care guidelines of the Institute of Laboratory Animal Resources of Nippon Veterinary and Life Science University, which conform to national guidelines, and international guidelines such as the ARRIVE guidelines.

Author contributions

Conceptualization, YY and TT; data curation, YY and TT; formal analysis, YY and TT; funding acquisition, TT; investigation, YY, TT, TN, MM, HS, YT, RS, and HM; methodology, YY and TT; project administration, YY and TT; resources, TT; supervision, TT; validation, YY and TT; visualization, YY and TT; writing—original draft, YY; writing—review and editing, TT, TN, MM, HS, YT, RS, and HM.

Funding

This work was financially supported by Research Center for Animal Life Science in Nippon Veterinary and Life Science University.

Declaration of competing interest

The authors declare that they have no known competing financial interests or personal relationships that could have appeared to influence the work reported in this paper.

Acknowledgments

The authors extend deep appreciation to Dr. Takuya Mizuno (Yamaguchi University, Japan) and Dr. Hirotaka Tomiyasu (University of Tokyo, Japan) for providing the cell lines used in this study. The authors also thank Angela Morben, DVM, ELS, from Edanz (https://jp.edanz.com/ac) for editing a draft of this manuscript.

Appendix A. Supplementary data

Supplementary data to this article can be found online at https://doi.org/10.1016/j.reth.2024.12.019.

References

[1] Kol A, Arzi B, Athanasiou KA, Farmer DL, Nolta JA, Rebhun RB, et al. Companion animals: translational scientist's new best friends. Sci Transl Med 2015;7:308ps21.
[2] Voga M, Adamic N, Vengust M, Majdic G. Stem cells in veterinary medicine-current state and treatment options. Front Vet Sci 2020;7:278.
[3] Rhee KJ, Lee JI, Eom YW. Mesenchymal stem cell-mediated effects of tumor support or suppression. Int J Mol Sci 2015;16:30015–33.
[4] Karnoub AE, Dash AB, Vo AP, Sullivan A, Brooks MW, Bell GW, et al. Mesenchymal stem cells within tumour stroma promote breast cancer metastasis. Nature 2007;449:557–63.
[5] Xu WT, Bian ZY, Fan QM, Li G, Tang TT. Human mesenchymal stem cells (hMSCs) target osteosarcoma and promote its growth and pulmonary metastasis. Cancer Lett 2009;281:32–41.
[6] Teshima T, Matsumoto H, Koyama H. Soluble factors from adipose tissue-derived mesenchymal stem cells promote canine hepatocellular carcinoma cell proliferation and invasion. PLoS One 2018;13:e0191539.
[7] Khakoo AY, Pati S, Anderson SA, Reid W, Elshal MF, Rovira II, et al. Human mesenchymal stem cells exert potent antitumorigenic effects in a model of Kaposi's sarcoma. J Exp Med 2006;203:1235–47.
[8] Jergens AE, Heilmann RM. Canine chronic enteropathy-current state-of-the-art and emerging concepts. Front Vet Sci 2022;9:923013.
[9] Dandrieux JRS, Mansfield CS. Chronic enteropathy in canines: prevalence, impact and management strategies. Vet Med (Auckl) 2019;10:203–14.
[10] Yasumura Y, Teshima T, Nagashima T, Michishita M, Taira Y, Suzuki R, et al. Effective enhancement of the immunomodulatory capacity of canine adipose-derived mesenchymal stromal cells on colitis by priming with colon tissue from mice with colitis. Front Vet Sci 2024;11:1437648.
[11] Cristóbal JI, Duque FJ, Usón-Casaús JM, Ruiz P, Nieto EL, Pérez-Merino EM. Effects of allogeneic mesenchymal stem cell transplantation in dogs with inflammatory bowel disease treated with and without corticosteroids. Animals (Basel) 2021;11:2061.
[12] Sogame N, Risbon R, Burgess KE. Intestinal lymphoma in dogs: 84 cases (1997-2012). J Am Vet Med Assoc 2018;252:440–7.
[13] Carrasco V, Rodríguez-Bertos A, Rodríguez-Franco F, Wise AG, Maes R, Mullaney T, et al. Distinguishing intestinal lymphoma from inflammatory bowel disease in canine duodenal endoscopic biopsy samples. Vet Pathol 2015;52:668–75.
[14] Coyle KA, Steinberg H. Characterization of lymphocytes in canine gastrointestinal lymphoma. Vet Pathol 2004;41:141–6.
[15] Fukushima K, Ohno K, Koshino-Goto Y, Uchida K, Nomura K, Takahashi M, et al. Sensitivity for the detection of a clonally rearranged antigen receptor gene in endoscopically obtained biopsy specimens from canine alimentary lymphoma. J Vet Med Sci 2009;71:1673–6.
[16] Lee MW, Ryu S, Kim DS, Lee JW, Sung KW, Koo HH, et al. Mesenchymal stem cells in suppression or progression of hematologic malignancy: current status and challenges. Leukemia 2019;33:597–611.

[17] Yasumura Y, Teshima T, Taira Y, Saito T, Yuchi Y, Suzuki R, et al. Optimal intravenous administration procedure for efficient delivery of canine adipose-derived mesenchymal stem cells. Int J Mol Sci 2022;23:14681.
[18] Umeki S, Ema Y, Suzuki R, Kubo M, Hayashi T, Okamura Y, et al. Establishment of five canine lymphoma cell lines and tumor formation in a xeno-transplantation model. J Vet Med Sci 2013;75:467–74.
[19] Momoi Y, Okai Y, Watari T, Goitsuka R, Tsujimoto H, Hasegawa A. Establishment and characterization of a canine T-lymphoblastoid cell line derived from malignant lymphoma. Vet Immunol Immunopathol 1997;59:11–20.
[20] Nakaichi M, Taura Y, Kanki M, Mamba K, Momoi Y, Tsujimoto H, et al. Establishment and characterization of a new canine B-cell leukemia cell line. J Vet Med Sci 1996;58:469–71.
[21] Roode SC, Rotroff D, Richards KL, Moore P, Motsinger-Reif A, Okamura Y, et al. Comprehensive genomic characterization of five canine lymphoid tumor cell lines. BMC Vet Res 2016;12:207.
[22] Meleshina AV, Cherkasova EI, Shirmanova MV, Klementieva NV, Kiseleva EV, Snopova LB, et al. Influence of mesenchymal stem cells on metastasis development in mice in vivo. Stem Cell Res Ther 2015;6:15.
[23] Ma Y, Hao X, Zhang S, Zhang J. The in vitro and in vivo effects of human umbilical cord mesenchymal stem cells on the growth of breast cancer cells. Breast Cancer Res Treat 2012;133:473–85.
[24] Tian K, Yang S, Ren Q, Han Z, Lu S, Ma F, et al. p38 MAPK contributes to the growth inhibition of leukemic tumor cells mediated by human umbilical cord mesenchymal stem cells. Cell Physiol Biochem 2010;26:799–808.
[25] Yuan Y, Chen D, Chen X, Shao H, Huang S. Human umbilical cord-derived mesenchymal stem cells inhibit proliferation but maintain survival of Jurkat leukemia cells in vitro by activating Notch signaling. Nan Fang Yi Ke Da Xue Xue Bao 2014;34:441–7.
[26] Panayiotidis P, Jones D, Ganeshaguru K, Foroni L, Hoffbrand AV. Human bone marrow stromal cells prevent apoptosis and support the survival of chronic lymphocytic leukaemia cells in vitro. Br J Haematol 1996;92:97–103.
[27] Nwabo Kamdje AH, Mosna F, Bifari F, Lisi V, Bassi G, Malpeli G, et al. Notch-3 and Notch-4 signaling rescue from apoptosis human B-ALL cells in contact with human bone marrow-derived mesenchymal stromal cells. Blood 2011;118:380–9.
[28] Maqsood MI, Matin MM, Bahrami AR, Ghasroldasht MM. Immortality of cell lines: challenges and advantages of establishment. Cell Biol Int 2013;37:1038–45.
[29] Taher L, Beck J, Liu W, Roolf C, Soller JT, Rütgen BC, et al. Comparative high-resolution transcriptome sequencing of lymphoma cell lines and de novo lymphomas reveals cell-line-specific pathway dysregulation. Sci Rep 2018;8:6279.
[30] Liang R, Huang GS, Wang Z, Chen XQ, Bai QX, Zhang YQ, et al. Effects of human bone marrow stromal cell line (HFCL) on the proliferation, differentiation and apoptosis of acute myeloid leukemia cell lines U937, HL-60 and HL-60/VCR. Int J Hematol 2008;87:152–66.
[31] Sarmadi VH, Tong CK, Vidyadaran S, Abdullah M, Seow HF, Ramasamy R. Mesenchymal stem cells inhibit proliferation of lymphoid origin haematopoietic tumour cells by inducing cell cycle arrest. Med J Malaysia 2010;65:209–14.
[32] Ahn JO, Chae JS, Coh YR, Jung WS, Lee HW, Shin IS, et al. Human adipose tissue-derived mesenchymal stem cells inhibit T-cell lymphoma growth in vitro and in vivo. Anticancer Res 2014;34:4839–47.
[33] Maylina L, Kambayashi S, Baba K, Okuda M. Simultaneous analysis of the p16 gene and protein in canine lymphoma cells and their correlation with pRb phosphorylation. Vet Sci 2022;9:393.
[34] Ema Y, Igase M, Takeda Y, Yanase T, Umeki S, Hiraoka H, et al. Investigation of the cytotoxic effect of flavopiridol in canine lymphoma cell lines. Vet Comp Oncol 2016;14:95–106.
[35] Maylina L, Kambayashi S, Baba K, Igase M, Mizuno T, Okuda M. Decreased sensitivity of cyclin-dependent kinase 4/6 inhibitors, palbociclib and abemaciclib to canine lymphoma cells with high p16 protein expression and low retinoblastoma protein phosphorylation. J Vet Med Sci 2023;85:99–104.
[36] Kobayashi K, Baba K, Kambayashi S, Okuda M. Blockade of isoprenoids biosynthesis by simvastatin induces autophagy-mediated cell death via downstream c-Jun N-terminal kinase activation and cell cycle dysregulation in canine T-cell lymphoma cells. Res Vet Sci 2024;169:105174.
[37] Song N, Gao L, Qiu H, Huang C, Cheng H, Zhou H, et al. Mouse bone marrow-derived mesenchymal stem cells inhibit leukemia/lymphoma cell proliferation in vitro and in a mouse model of allogeneic bone marrow transplant. Int J Mol Med 2015;36:139–49.
[38] Li Q, Pang Y, Liu T, Tang Y, Xie J, Zhang B, et al. Effects of human umbilical cord-derived mesenchymal stem cells on hematologic malignancies. Oncol Lett 2018;15:6982–90.
[39] Ramasamy R, Lam EW, Soeiro I, Tisato V, Bonnet D, Dazzi F. Mesenchymal stem cells inhibit proliferation and apoptosis of tumor cells: impact on in vivo tumor growth. Leukemia 2007;21:304–10.
[40] Tian LL, Yue W, Zhu F, Li S, Li W. Human mesenchymal stem cells play a dual role on tumor cell growth in vitro and in vivo. J Cell Physiol 2011;226:1860–7.
[41] Zhu Y, Sun Z, Han Q, Liao L, Wang J, Bian C, et al. Human mesenchymal stem cells inhibit cancer cell proliferation by secreting DKK-1. Leukemia 2009;23:925–33.
[42] Secchiero P, Zorzet S, Tripodo C, Corallini F, Melloni E, Caruso L, et al. Human bone marrow mesenchymal stem cells display anti-cancer activity in SCID mice bearing disseminated non-Hodgkin's lymphoma xenografts. PLoS One 2010;5:e11140.
[43] Harrell CR, Volarevic A, Djonov VG, Jovicic N, Volarevic V. Mesenchymal stem cell: a friend or foe in anti-tumor immunity. Int J Mol Sci 2021;22:12429.
[44] Lee MJ, Park SY, Ko JH, Lee HJ, Ryu JS, Park JW, et al. Mesenchymal stromal cells promote B-cell lymphoma in lacrimal glands by inducing immunosuppressive microenvironment. Oncotarget 2017;8:66281–92.
[45] Lu YR, Yuan Y, Wang XJ, Wei LL, Chen YN, Cong C, et al. The growth inhibitory effect of mesenchymal stem cells on tumor cells in vitro and in vivo. Cancer Biol Ther 2008;7:245–51.
[46] Lin HD, Fong CY, Biswas A, Bongso A. Hypoxic Wharton's Jelly stem cell conditioned medium induces immunogenic cell death in lymphoma cells. Stem Cells Int 2020;2020:4670948.
[47] Barcellos-de-Souza P, Comito G, Pons-Segura C, Taddei ML, Gori V, Becherucci V, et al. Mesenchymal stem cells are recruited and activated into carcinoma-associated fibroblasts by prostate cancer microenvironment-derived TGF-β1. Stem Cell 2016;34:2536–47.
[48] Mele V, Muraro MG, Calabrese D, Pfaff D, Amatruda N, Amicarella F, et al. Mesenchymal stromal cells induce epithelial-to-mesenchymal transition in human colorectal cancer cells through the expression of surface-bound TGF-β. Int J Cancer 2014;134:2583–94.
[49] Lindoso RS, Collino F, Camussi G. Extracellular vesicles derived from renal cancer stem cells induce a pro-tumorigenic phenotype in mesenchymal stromal cells. Oncotarget 2015;6:7959–69.
[50] Goldstein RH, Reagan MR, Anderson K, Kaplan DL, Rosenblatt M. Human bone marrow-derived MSCs can home to orthotopic breast cancer tumors and promote bone metastasis. Cancer Res 2010;70:10044–50.
[51] Clarke MR, Imhoff FM, Baird SK. Mesenchymal stem cells inhibit breast cancer cell migration and invasion through secretion of tissue inhibitor of metalloproteinase-1 and -2. Mol Carcinog 2015;54(10):1214–9.
[52] Chen HL, Li JJ, Jiang F, Shi WJ, Chang GY. MicroRNA-4461 derived from bone marrow mesenchymal stem cell exosomes inhibits tumorigenesis by down-regulating COPB2 expression in colorectal cancer. Biosci Biotechnol Biochem 2020;84:338–46.
[53] Li GC, Ye QH, Xue YH, Sun HJ, Zhou HJ, Ren N, et al. Human mesenchymal stem cells inhibit metastasis of a hepatocellular carcinoma model using the MHCC97-H cell line. Cancer Sci 2010;101:2546–53.
[54] Schelter F, Halbgewachs B, Bäumler P, Neu C, Görlach A, Schrötzlmair F, et al. Tissue inhibitor of metalloproteinases-1-induced scattered liver metastasis is mediated by hypoxia-inducible factor-1α. Clin Exp Metastasis 2011;28:91–9.
[55] Yamazaki H, Tanaka T, Nishida H, Hatoya S, Akiyoshi H. Hypoxia-targeting therapy for intestinal T-cell lymphoma in dogs: preclinical study using 3D in vitro models. Vet Comp Oncol 2023;21:12–9.
[56] Yamazaki H, Tanaka T, Nishida H, Hatoya S, Akiyoshi H. Assessment of hypoxia-targeting therapy for gastrointestinal lymphoma in dogs: preclinical test using murine models. Res Vet Sci 2023;154:22–8.
[57] Kanei T, Iwata M, Kamishina H, Mizuno T, Maeda S. Expression and functional analysis of chemokine receptor 7 in canine lymphoma cell lines. J Vet Med Sci 2022;84:25–30.